BB

GSI PRE 94-38
SW 9429

GSI

GSI-94-38
PREPRINT
JUNI 1994

BETA DECAY OF NEUTRON-DEFICIENT EVEN-MASS INDIUM ISOTOPES: EVIDENCE FOR POPULATION OF HIGHLY-EXCITED STATES IN THE CADMIUM DAUGHTER NUCLEI

J. SZERYPO et al.

CERN LIBRARIES, GENEVA
P00024414

Gesellschaft für Schwerionenforschung mbH
Postfach 110552 · D-64220 Darmstadt · Germany

Beta decay of neutron-deficient even-mass indium isotopes: evidence for population of highly-excited states in the cadmium daughter nuclei

J. Szerypo[1,*], M. Huyse[1], G. Reusen[1], P. Van Duppen[1], Z. Janas[2,*], H. Keller[2], R. Kirchner[2], O. Klepper[2], A. Piechaczek[2], E. Roeckl[2], D. Schardt[2], K. Schmidt[2], R. Grzywacz[3], M. Pfützner[3], A. Płochocki[3], K. Rykaczewski[3], J. Żylicz[3], G. Alkhazov[4], L. Batist[4], A. Bykov[4], V. Wittmann[4] and B. A. Brown[5]

[1] Instituut voor Kern- en Stralingsfysica, K.U. Leuven, B-3001 Leuven, Belgium

[2] Gesellschaft für Schwerionenforschung, D-64220 Darmstadt, Germany

[3] Institute of Experimental Physics, Warsaw University, PL-00-681 Warsaw, Poland

[4] St. Petersburg Nuclear Physics Institute, 188350 Gatchina, Russia

[5] NSCL, Dept. of Physics and Astronomy, Michigan State University, East Lansing, Michigan, 48824-1321, USA

Keywords:

RADIOACTIVITY ^{100,102,104}In (EC), (β^+) [from ^{50}Cr(^{58}Ni,xn3p), E=5.6 MeV/nucleon]; measured E_γ, I_γ, E_p, I_p, E_β, pγ-, $\beta\gamma$-, $\gamma\gamma$-coin, $T_{1/2}$; deduced B(GT), ^{102}In levels.

Ge, Si detectors. On-line mass separation.

---

* On leave of absence from the Institute of Experimental Physics, Warsaw University, PL-00-681 Warsaw, Poland

Abstract

By using mass-separated sources, positrons as well as β-delayed protons and γ rays were measured from the β decay of ^{102}In ($T_{1/2}$ = 22 ± 1 s) and ^{100}In ($T_{1/2}$ = 6.1 ± 0.9 s). In particular, the average $\beta^+/(\beta^+ + EC)$ ratio for the decay of ^{102}In was measured to be 0.76 (4) and a detailed level scheme of ^{102}Cd was constructed. Whereas no direct β^+/EC feeding of the identified ^{102}Cd levels was observed, there is evidence for population of ^{102}Cd states at high excitation energy followed by statistical γ decay. This feature, which has been deduced on the basis of the measured positron spectrum and the measured $\beta^+/(\beta^+ + EC)$ ratio of the ^{102}In decay, is compared to the decay properties of the heavier odd-odd indium isotopes ^{104}In, ^{106}In and ^{108}In, and is also used to interpret the observed β-delayed proton data of ^{102}In and ^{100}In. For the first time, large-space shell-model calculations have been performed for the Gamow-Teller decay of heavy odd-odd nuclei. The decay results from these calculations are in good overall agreement with the gross decay properties of ^{102}In and ^{100}In deduced from the experiment.

1. Introduction

The ß$^+$/EC decay of neutron-deficient isotopes near the doubly-magic nucleus ^{100}Sn is dominated by the Gamow-Teller (GT) transformation of a $g_{9/2}$ proton into a $g_{7/2}$ neutron. Within the framework of the extreme single-particle shell model, the ground state configurations of ^{100,102,104}In result from the coupling of an odd $g_{9/2}$ proton to an odd $d_{5/2}$ neutron. Therefore, in the decay of these nuclei one would expect that: (i) a two-neutron quasiparticle state ($\nu d_{5/2}$, $\nu g_{7/2}$) at an excitation energy of 2 to 3 MeV in the cadmium daughter could be populated via a direct transformation of a $g_{9/2}$ proton into a $g_{7/2}$ neutron [1]; (ii) the decay of the even-even part of the indium core could lead to a four-quasiparticle structure in the cadmium daughter at an excitation energy of about 5 to 6 MeV; this state would be composed of a GT pair ($\pi g_{9/2}^{-1}$,$\nu g_{7/2}$) coupled to 1^+ and two odd particles, namely $\pi g_{9/2}$ and $\nu d_{5/2}$.

A decay study of ^{104}In [2,3] reported a strong ß$^+$/EC feeding to high-lying levels in ^{104}Cd : 70 % of the total ß$^+$/EC decay feeds the levels with an excitation energy above 5 MeV, while in the previously proposed decay scheme [4] 100 % of the ß$^+$/EC decay populated the states below 3.5 MeV. The subsequent γ decay from these high-lying levels is of statistical character, involves cascades of high multiplicity and can not be resolved by discrete γ spectroscopy. This makes standard spectroscopic methods unreliable : it is impossible to extract the ß feeding from the intensity balance of discrete γ rays, i.e. from taking feeding and deexciting transitions for a given level into account. Therefore alternative methods have to be used to deduce the gross structure of the ß-strength function. In reference [5], this was achieved for the ^{104}In decay on the basis of measured positron spectrum and ß$^+$/(ß$^+$+EC) ratio. These measurements indicate a shift of the ß strength function to higher energies; this shift has meanwhile been confirmed by means of a total absorption gamma spectrometer (TAGS) [1,6].

It was expected that this remarkable ß$^+$/EC feeding of high-energy levels should also influence the decay properties of the lighter odd-odd indium isotopes. In order to clarify this question we investigated the β decay of ^{102}In and ^{100}In. In presenting the results from this

study we proceed in the following way. After describing the experimental techniques (Section 2), we present the experimental results (Section 3) obtained from measuring X rays and β-delayed γ rays, positrons, $\beta^+/(\beta^+ + EC)$ ratios and β-delayed protons. The discussion (Section 4), which focuses on the deduced $^{102}In \rightarrow {}^{102}Cd$ level scheme and on the β strength function measured for the decays of $^{102,104,106,108}In$, takes experimental data on the GT-strength of neighboring nuclei as well as a shell-model calculation into account. Section 5 contains our conclusions.

2. Experimental techniques

^{102}In and ^{100}In were produced via the $^{50}Cr(^{58}Ni,3p3n)$ and $^{50}Cr(^{58}Ni,3p5n)$ reactions, respectively. A 5.6 MeV/u ^{58}Ni beam of about 30 to 50 particle-nA from the linear accelerator UNILAC at GSI Darmstadt impinged on an enriched ^{50}Cr target (3.5 mg/cm^2, enrichment 97%, 2.1 mg/cm^2 Mo backing) which was mounted close to the ion source of the GSI On-line Mass Separator. Two types of ion sources were used. The first one was a FEBIAD-B2C ion source [7], yielding mass-separated beam intensities (per 40 particle-nA of ^{58}Ni) of 1440 atoms/s for ^{102}In and 10^5 atoms/s for ^{102}Ag. An example of a γ ray spectrum measured with this source is shown in Fig. 1a. In the previous work [8] the ratio between ^{102}Ag and ^{102}In intensities was more than an order of magnitude higher, causing difficulties in the identification of the ^{102}In activity. This is due to the large difference between the production cross-sections of the reactions $^{92}Mo(^{14}N,2p2n)^{102}Ag$ and $^{92}Mo(^{14}N,4n)^{102}In$ that were used in ref.[8]. This difference is considerably smaller for the reactions $^{50}Cr(^{58}Ni,5pn)^{102}Ag$ and $^{50}Cr(^{58}Ni,3p3n)^{102}In$ used in the present work.

The second ion source was a thermal ion source [9] delivering an almost pure ^{102}In beam with only a very small admixture of ^{102}Ag. The high chemical selectivity of the thermal ion source arises from differences in the ionization potentials which are 5.8 eV for indium, 9.0 eV for cadmium and 7.6 eV for silver. However, this gain in purity (see Fig. 1b) was achieved

at the expense of a loss in ^{102}In beam intensity which decreased by a factor of 9 compared to the FEBIAD ion source.

Five different collector-detector configurations were used to study the ß decay of ^{102}In and ^{100}In:

a) The mass-separated beam was switched between two carbon foils in order to study the grow-in/decay pattern of the implanted β-delayed proton activity by means of ΔE-E telescopes mounted close to the foils. A large Ge detector (70% relative efficiency) was placed at a distance of 150 mm to avoid summing effects.

b) The mass-separated atoms were implanted into a tape and moved periodically to a counting station equipped with a ΔE-E telescope, two large volume Ge (40 % and 70 % relative efficiencies) and a LEGe (Low Energy Germanium) detectors in close geometry.

c) Alternatively to b), the counting station was equipped with a 30 % Ge detector placed in close geometry (51 mm from the source) and a 90 % Ge detector in far geometry (144 mm from the source), the latter one being shielded from the background radiation by lead. In this set-up an annihilator (1 cm thick aluminum) surrounded the source to stop the beta particles in a small volume in order to have a well-defined efficiency for the 511 keV annihilation adiation.

d) As an alternative to b) and c), a summation-free ß$^+$-endpoint spectrometer [10] was used at the counting station to measure the energy spectrum of emitted positrons and the γ ray multiplicity.

e) Finally, some information on the β strength function for ^{104}In and the ß$^+$/(ß$^+$+EC) ratio for ^{102}In has been obtained with the Total Absorption Gamma Spectrometer (TAGS). The description of this detection system, together with results obtained for the decay of ^{100}Ag and ^{104}In, are given elsewhere [6].

The ΔE-E telescopes consisted of a 150 mm^2, 16-32 μm fully depleted and a 450 mm^2, 530-750 μm partially depleted silicon detectors. The detection efficiency of the telescopes ranged from 10 to 18% for the different detector arrays. These telescopes were water-cooled and held at a constant temperature of 14 °C. Both ΔE and E detectors were energy calibrated by inserting α sources. The mass dependence of the creation of particle-hole pairs in the silicon detector [11,12], which leads to a difference in energy calibration between the alpha particles

and protons, was taken into account. ΔE-E as well as ΔE-E-γ-t coincidence events were stored together with the time elapsed since beam switching (array a)) or tape transport (array b)).

The Ge detectors and the LEGe detector were operated in singles and coincidence mode. These detectors were energy calibrated using the known γ rays belonging to the decay of ^{102}Ag [13] and ^{102}Cd [14]. The absolute photopeak γ efficiency curves were measured using point-like calibrated sources. Due to summing effects occurring with positrons, 511 keV quanta and in particular with coincident γ ray cascades of high multiplicity (see Section 1), the γ spectra measured by close-geometry detectors are distorted and were therefore used only for determining accurate transition energies, and assigning weak γ lines, gaining coincidence information, whereas singles γ ray intensities were determined from spectra measured in far geometry. The absolute efficiency of the far-geometry detectors was below 1 % in the maximum of the energy-dependent yield curve and was thus about an order of magnitude lower than of the close-geometry ones.

3. Experimental results

3.1 X rays and β-delayed gamma rays from the decay of ^{102}In

The assignment of four γ rays and the tentative assignment of two additional γ rays to the decay of ^{102}In [8] has previously been based on the comparison between ^{92}Mo + ^{12}C in-beam γ data and γ data obtained from mass-separated sources by using ^{92}Mo + ^{14}N reaction. Tréherne et al. [8] were unable to establish a detailed decay scheme of ^{102}In due to the strong ^{102}Ag contamination. However, they assigned the 593.3 - 861.5 - 776.5 keV γ lines to be a ΔI = 2 cascade of stretched E2 transitions linking the 6^+-4^+, 4^+-2^+ and 2^+-0^+ states, respectively. The order of the 776.5 keV and 861.5 keV transitions might as well be reversed. From the intensity balance Tréherne et al. concluded that the spin of the ^{102}In ground state should not be smaller than 5.

A detailed analysis of our coincidence and singles data lead to the identification of 15 γ rays belonging to the β^+/EC decay of ^{102}In. All these γ rays were placed in a level scheme based on coincidence relations (see Fig. 2a). The sequence 861.5 - 776.5 keV was unambiguously determined by a cross-over transition between the 2035.3 keV and the 776.5 keV level.

The energies and relative intensities of the γ transitions appearing in the level scheme of Fig. 2a are listed in Table 1. They represent weighted averages of the values obtained with different detectors (the LEGe spectrum was recorded up to 800 keV). Because background radiation and, in particular, in case of the FEBIAD data, isobaric contaminations may interfere in the singles spectra, the γ ray intensity of the 822.4, 861.5, 1236.4 and 1258.8 keV lines was determined from the K_α X ray-gated or 776.5 keV-gated γ spectra. Since, as will be shown later, the multiplicity for all these γ rays is similar, the influence of summing on the relative intensities is small (for both far and close geometry, both singles and coincident spectra) and was disregarded. In addition, the intensity of the 861.5 keV line was determined from the isotopically pure spectra obtained with the thermal ion source. These data were also used to investigate the possibility of direct γ decay to the ground state of ^{102}Cd. Due to the high chemical selectivity of the thermal ion source, the ^{102}Cd activity observed in these spectra essentially stems from the decay of ^{102}In. By comparing with the set-up a) (where the summing effect had negligible influence also on the absolute intensity) the intensity of the 776.5 keV $2^+ - 0^+$ transition in the decay of ^{102}In with the 481.0 keV line in the decay of ^{102}Cd (see Fig. 1b)), 95 (7) % of the cadmium activity can be explained. This estimate, which does not depend on any assumption on β strength or γ deexcitation, leaves little room for direct γ decay to the ^{102}Cd ground state and indicates that, under the assumption of negligible direct β^+/EC decay to the ^{102}Cd ground state, the γ intensity values compiled in Table 1 can approximately be taken to represent intensities per β^+/EC decay.

The half-life of ^{102}In has been deduced by using the γ rays of 397.3, 593.3, 749.4 and 776.5 keV. A weighted average, based on different detectors and cycle times, yields $T_{1/2}$ = 22 (1) s, which is in agreement with the previously reported value of 24 (4) s [8].

At this point, the next step of standard γ ray spectroscopy analysis would consist of

(i) performing the γ ray intensity balance, i.e. calculating the intensity difference between the γ rays deexciting a level and those feeding it, and (ii) ascribing this difference to the direct ß feeding of the considered level. The missing intensities for the excited ^{102}Cd levels are given in Table 2. If the missing intensity would be due to ß feeding, one would expect that each level is characterized by a distinct β^+/EC ratio and a distinct γ ray multiplicity. We shall discuss $\beta^+/(\beta^+ + EC)$ ratios below (Section 3.3). Relevant to the question of the level-specific γ ray multiplicity is the observation that irrespective of the gating condition (γ rays, annihilation radiation or X rays) the relative γ ray intensities of the coincidence spectra are identical to those of the singles spectra (see ref. [15] and Table 3). This result indicates that the β-γ decay path to all observed levels must be similar. Therefore, the missing feeding cannot be related to level-specific β branching ratios, but has to be assigned to γ feeding that stems from highly excited levels; the statistical character of this γ deexcitation evidently prevents its detection in the Ge detectors which are characterized by a low-eficiency and by a resolution lower than the level spacing.

Qualitative information about the γ ray multiplicity was found by comparing the absolute γ ray intensity in the singles spectrum and in the total coincidence projection (detector configuration (b), FEBIAD ion source). A γ ray belonging to a high-multiplicity cascade is characterized by a smaller ratio between singles and coincidence intensities than a γ ray belonging to a low-multiplicity cascade. Such ratios are compiled in Table 3 for the decay of ^{102}Cd and ^{102}In. For ^{102}Cd the ratio varies as expected : the 481.0 keV transition has lower multiplicity than, e.g., the 360.6 keV transition and, correspondingly, higher singles/coincidence ratio. For the ^{102}In decay, however, this ratio stays rather constant and is much lower than in case of ^{102}Cd. This observation indicates that the multiplicity for ^{102}In is much higher than for all investigated ^{102}Cd γ rays, but almost identical for all observed ^{102}In γ rays. Such an analysis does not give an exact number for the multiplicity. However, this number can be extracted from data collected with the summation-free β^+-endpoint spectrometer which allows one to use the segments of a BGO ring for multiplicity determination. The resulting multiplicity of approximately 5 γ rays per decay, excluding the

EC X rays or the two 511 keV quanta from β^+ annihilation, is identical to that of ^{104}In [2,3] and fits also to the preliminary results from the TAGS data analysis [6].

3.2 Positron spectrum from the decay of ^{102}In

As an alternative to the method of studying the missing γ ray intensity described in Section 3.1, one may obtain the gross structure of the ß-strength function from the deconvolution of the measured ß spectrum [5]. In our experiment, the spectrum originating from the decay of ^{102}In was measured with the summation-free β^+-endpoint spectrometer [10]. Unfortunately counting statistics was rather poor (the ^{102}In ß spectrum was actually measured as a byproduct in the β^+-endpoint measurement of ^{102}Cd [14]) so that an unambiguous determination of the β strength from a deconvolution of the measured spectrum was impossible. Nevertheless the ß spectrum, displayed in Fig. 3, can be used to get some qualitative information on the ß strength. While the extrapolated value of Q_{EC} for ^{102}In is 8.90 (33) MeV [16], the measured β^+ spectrum ends at 3.5 (5) MeV. This indicates the existence of substantial ß feeding to levels between 4 MeV and the Q_{EC} value. The lower-lying states, presented in the level scheme of ^{102}Cd (see Fig. 2a), receive less than 10 % of the direct β^+ feeding. This result confirms the conclusion drawn from the γ data on the dominant feeding of high-lying ^{102}Cd states (see Section 3.1).

3.3 $\beta^+/(\beta^+$+EC) ratio for the decay of ^{102}In and ^{104}In

Another method to deduce information about the strength distribution in β^+/EC decay is the use of the $\beta^+/(\beta^+$+EC) ratio. In ref. [5], this ratio was deduced for ^{104}In from the deconvolution of the positron spectrum and from the comparison between the β^+ and γ ray intensities. Due to the low statistics in the positron spectrum of ^{102}In, these methods cannot be applied here. However, the ratio can also be determined by comparing the intensities of the

511 keV line and the $2^+ - 0^+$ γ transition in ^{102}Cd (776.5 keV). Both lines were measured in one and the same detector in order to reduce systematic errors. The set-up (c) equipped with the annihilator was used. The β^+ particles were stopped in the small volume of the annihilator and, after a correction for annihilation in flight (5 ± 5 % probability), the β^+ intensity was derived from the measured 511 keV intensity. Gating on the $4^+ - 2^+$ transition in ^{102}Cd, observed in the close-geometry detector, a $\beta^+/(\beta^+ + EC)$ ratio of $0.91^{+0.09}_{-0.11}$ was deduced from the γ intensities at 511 and 776.5 keV, determined by means of the far-geometry detector. In this evaluation, possible unobserved transitions to the ^{102}Cd ground state were taken into account by assuming an intensity of 95 (7) % for the 776.5 keV transition (see Section 3.1). The gating condition filters out the ^{102}Cd and ^{102}Ag contamination, present in the mass-102 samples prepared by using the FEBIAD ion source and hence contributing to the 511 keV line.

As an alternative to the coincidence method, the contribution of isobaric contaminants to the 511 keV intensity can be disentangled by analyzing the single spectra recorded in a multispectrum mode. This yields a $\beta^+/(\beta^+ + EC)$ ratio of 0.72 (7) using the $2^+ \rightarrow 0^+$ transition in ^{102}Cd, taking again corrections for positron annihilation in flight and for direct γ decay to the ^{102}Cd ground state into account. The evaluation of TAGS data results in a $\beta^+/(\beta^+ + EC)$ ratio of 0.75 (5) [6]. We shall use the weighted average of the three measured $\beta^+/(\beta^+ + EC)$ ratios, i.e. 0.76 (4), in the following discussion.

In order to check the procedures applied for determining $\beta^+/(\beta^+ + EC)$ ratios, the ^{104}In decay was reinvestigated. The coincidence method yielded a $\beta^+/(\beta^+ + EC)$ ratio of 0.44 (3), whereas a value of 0.45 (1) was obtained from the singles spectra measured by using the thermal ion source. These results are in good agreement with (i) those reported earlier [5], namely 0.48 (3) from the β^+ spectrum and 0.54 (6) from comparing 511 keV and $2^+ - 0^+$ transition intensities, and (ii) the preliminary TAGS result of 0.45 (2) [1,6]. On the basis of the TAGS data, we also redetermined the half-life of ^{104}In to be 108 (2) s, confirming the previous value 108 (12) s of [17]. This data will be used below for deriving the GT strength (see Section 4.2).

3.4 Beta-delayed proton emission from the decay of ^{102}In and ^{100}In

The β-delayed proton data, deduced from the measurements of ^{102}In and ^{100}In decays, are compiled in Table 4, which includes also a comparison with results from a recent mass evaluation and from model calculations. By using the FEBIAD ion source and the collector-detector arrays a) and b), the proton spectra displayed in Fig. 4 were obtained and the half-lives of ^{102}In and ^{100}In were determined to be 24 ± 3 s and 6.1 ± 0.9 s, respectively, from a time analysis of the proton activity. The value of 24 ± 3 s agrees with the more accurate one (22 ± 1 s) deduced from γ ray data (see Section 3.1). The β-delayed proton activity of ^{100}In has first been observed by Kurcewicz et al. [18], who were unable to determine its half-life or to obtain a proton energy spectrum. On the basis of the p-γ and p-X coincidence data (see Fig. 5), the probability ratio $(ß^+/(ß^+{+}EC))_{\beta p}$ was found to be 0.07 ± 0.07 and $0.80^{+0.14}_{-0.11}$ for ^{102}In and ^{100}In, respectively. These ratios characterize β decay to proton-emitting states only and should not be confused with the total $ß^+/(ß^+{+}EC)$ ratios discussed in Section 3.3.

From the measured proton spectra and the $(ß^+/(ß^+{+}EC))_{\beta p}$ ratios, Q_{EC} limits have been deduced (see Table 4). A lower limit was obtained by summation of the highest proton energy observed for ^{102}In (detector array b)) and ^{100}In (detector array a)), i.e. 3.32 ± 0.05 MeV and 4.70 ± 0.05 MeV (see Fig. 4), and the known [16] proton separation energy of ^{102}Cd and ^{100}Cd, respectively. An upper limit was determined (detector array b)) on the basis of the known energy dependence of the EC/$β^+$ ratio [19] under the assumptions that the measured $(ß^+/(ß^+{+}EC))_{\beta p}$ is due to proton emission to the ground state of the final nucleus (^{101}Ag, ^{99}Ag).

The total branching ratio $b_{\beta p}$ for β-delayed proton emission was determined from the simultaneous measurement of γ-singles and proton spectra under the assumption that all β decays of ^{102}In and ^{100}In pass through the $2^+ \rightarrow 0^+$ transitions of 776.5 and 1004 keV in ^{102}Cd and ^{100}Cd [20,21], respectively (see Sections 3.1 to 3.3 for the discussion of the ^{102}In → ^{102}Cd case). This experiment, which was performed by using the thermal ion source and detector array a), allowed us to determine a $b_{\beta p}$ value of $(9.3 \pm 1.3)\cdot 10^{-5}$ for ^{102}In,

whereas, due to the non-observation of the 1004 keV γ line, only a lower $b_{\beta p}$ limit was deduced for ^{100}In (see Table 4). From the p-γ coincidence measurements, proton emission to the first excited state of ^{101}Ag at 98 keV [22] has been established with a branching ratio (relative to $b_{\beta p}$) $b_{\beta p}^{exc}$ of 19 (9) %, whereas the search for the population of the 343 keV state in ^{99}Ag [23] remained unsuccessful (see Table 4).

4. Discussion

4.1 The ^{102}In → ^{102}Cd level scheme

The ^{102}In → ^{102}Cd level scheme obtained in this work (see Fig. 2a) includes 7 new energy levels and 9 new γ transitions compared to the previously published decay data [8] and shows also a perfect agreement with in-beam data [8] up to an excitation energy of 3 MeV (see Fig. 2b). The 822.0 keV transition, deexciting the 3053.7 keV level with probable spin and parity 8^+, is clearly present in our decay data, while the 269.3 keV transition, deexciting the 2987.4 keV level with a probable spin 7 or 9, has not been observed. The tentative spin and parity assignment of 8^+ for the level at 3053.7 keV has already been proposed in [20].

Fig. 6 shows the systematics of the low-energy part of the level schemes of even-even cadmium isotopes with masses ranging from 100 to 110. All displayed levels, except those of ^{100}Cd, have been observed in the β^+/EC decay of the high-spin states of the odd-odd indium mother nuclei, which represent the ground states of ^{102}In, ^{104}In and ^{106}In and the isomeric states of ^{108}In and ^{110}In. The levels of ^{100}Cd have been identified in in-beam studies [20,21].

The decay studies clearly become less complete when going from ^{110}In to ^{102}In : the relative intensity of the weakest γ ray placed in the level scheme increases from 0.12 % for ^{110}In to 1.7 % for ^{102}In. This deficiency will certainly play an important role in the high-energy part of the level scheme but is less important in the displayed low-energy part. The excitation energy, spin and parity of the $^{100\text{-}110}$Cd levels given in Fig. 6 show a systematic behavior which reflects the transition from collective (vibrational) to spherical shell structure

with decreasing neutron number. The increase of the 2^+ level energy and the decrease of the level splitting with decreasing mass number indicate the influence of the N=50 closed shell.

It is interesting to note that the 8^+ and 6^+ levels in the even-A cadmium isotopes are fed directly in the decay of $I^\pi = 7^+$ ground states of ^{110}In and ^{108}In, whereas the decay of ^{104}In and ^{102}In (probable ground state spin and parity 6^+ or 7^+) populates higher-lying levels which subsequently feed the 8^+ and 6^+ levels in a sequence of $\Delta I = 0, 1$ transitions, while ^{106}In takes an intermediate position (see refs. in Fig.6 caption). The observed decay pattern of ^{102}In does not allow for a ground state spin/parity assignment of 5^+, which was suggested [8] by assuming the direct feeding to the 4^+ excited state. As will be discussed below, shell-model calculations [24] favor a $I^\pi = 6^+$ assignment for the ground state of ^{102}In.

4.2 ß-strength function of even-A indium isotopes

Despite the fact that the deconvolution of the $ß^+$ spectrum was not possible, the β strength of ^{102}In can be approximately derived from the measured $ß^+/(ß^+ + EC)$ ratio. It is clear that the $ß^+/(ß^+ + EC)$ ratio of 0.76 (4), measured for the ^{102}In decay, qualitatively indicates β feeding of highly excited ^{102}Cd states, since one would expect $ß^+/EC$ ratios [19] of 48 and 22 for direct β feeding of the ^{102}Cd states at excitation energies of 1638 and 3054 keV, respectively. One way to gain quantitative information on the gross structure of the β strength function is to define the so called "100 % level". This is a fictitious level in the daughter nucleus which takes the entire beta feeding. The excitation energy of this level is defined by the condition that the $ß^+/(ß^+ + EC)$ ratio agrees with the experimentally determined value. The energy difference between the excitation energy $E_{100\%}$ of this "100 % level" and the Q_{EC} value can be found by using the tables of Gove and Martin [19] which give the $ß^+/EC$ ratio as a function of the beta energy. The strength concentrated in the β transition to the "100 % level" can then, where possible, be compared with the experimentally obtained beta strength function. Fig. 7 gives this "100 % level" as well as GT strength function B(GT) for the decay of the odd-odd nuclei $^{100\text{-}108}$In. In case of ^{106}In, the "100% level" was determined by using a

$\beta^+/(\beta^+ + EC)$ ratio of 0.36 (9), measured from the ratio between the intensities of X rays and $2^+ - 0^+$ ^{106}Cd transitions [25]. For ^{106,108}In, B(GT) was deduced from the γ intensity balance [26,27]. For ^{104}In, B(GT) was derived from a preliminary deconvolution of the TAGS spectrum [1,6]. Even though the application of the deconvolution method to the ^{104}In data faced some inconsistencies [6], the derived strength function agrees with results obtained previously [5,28]. The GT strength is calculated by using the relation [29]:

$$B(GT) = \frac{3862}{ft} s \qquad (1)$$

and is given in units of $g_A^2 / 4\pi$. The summed GT strength, $B_\Sigma(GT)$, taken as the sum of the partial GT strengths for the different energy bins, can then be used to calculate, on the basis of equation (1), the corresponding value of $\log(ft)_\Sigma$, with $\log(ft)_{100}$ being defined as the log(ft) value resulting from a (fictitious) concentration of the ß feeding in the "100 % level". The "100 % level" for ^{104}In lies well inside the measured ß strength distribution while for ^{106}In it lies on the edge of the experimental distribution. This means that already in the decay of ^{106}In ß strength is missing at higher excitation energy and that some of the assumed ß feeding [26] is due to unobserved γ rays.

Based on the tables of Gove and Martin [19], it can be shown that $\log(ft)_{100}$ is always higher than the $\log(ft)_\Sigma$ of any broader strength distribution and thus forms an upper limit for $\log(ft)_\Sigma$, whereas the GT strength corresponding to $\log(ft)_\Sigma$ represents a lower limit. This is the case for ^{104}In but clearly not for ^{106}In, which again indicates that there is strength missing in the published decay scheme of ^{106}In [26]. From the $\beta^+/(\beta^+ + EC)$ ratio of 0.76 (4), measured for the decay of ^{102}In, a $\log(ft)_{100}$ equals to $3.44^{+0.14}_{-0.13}$ and a corresponding GT strength of $1.4^{+0.5}_{-0.4}$ was deduced.

Fig. 8 displays the $B_\Sigma(GT)$ values for nuclei in the neighborhood of ^{100}Sn [30]. The trend emerging from this compilation is that the summed strength increases when approaching ^{100}Sn, independent upon whether an isotopic, isotonic or isobaric approach is chosen. Applying this to ^{102}In means that the summed GT strength is probably even higher than 1.9,

the value for ^{104}In [6], and that the strength determined for the "100 % level" of ^{102}Cd indeed represents only a lower limit.

Further insight into the β-decay near ^{100}Sn can be gained by comparing the measured half-life and the measured β-delayed proton data of ^{102}In and ^{100}In with predictions from the shell-model calculations [24]. For both nuclei ground state spin/parity assignments of 6^+ and 7^+ were assumed as suggested by these calculations. Taking into account the retardation of GT transition due to the core polarization (hindrance factor h_{cp}=1.66 [31]) and higher order effects (h_{ho}=1.6 [29,32]) the total GT strength for the decay of ^{102}In, predicted to appear within the calculated Q_{EC} window of 8.7 MeV (see Fig. 7), is about 5.0. Over 98% of the total calculated strength, corresponding to more than 75% of the β^+/EC intensity, populates the states above 4 MeV excitation energy and forms a broad resonant structure with a maximum at about 5.6 MeV, which is very close to the $E_{100\%}$ value of 5.74 MeV derived from experiment (see Fig. 7d). The GT strength distribution calculated for the decay of ^{100}In (see Fig. 7e) has similar features as that for ^{102}In. The β decay half-lives, predicted for ^{102}In and ^{100}In, are 10 and 5 s, respectively. While the theoretical $T_{1/2}$ for ^{100}In is in fair agreement with the experimental result of 6.1 (9) s, the ^{102}In decay ($T_{1/2}$ = 22 (1) s) is retarded by factor of 2 compared to the calculations. A similar feature is observed when comparing the theoretical $T_{1/2}$ results for ^{98}Cd (8.4 s)and ^{100}Cd (30 s) to the measured values of 9.2 (3) s [33] and 49.1 (5) s [34], respectively. The theory accounting for h_{cp} and h_{ho} hindrance factors fits well to the half-life of N=50 and 51 parent nuclei, and yields too small $T_{1/2}$ values for the heavier nuclei. This might be an indication that h_{cp} should be N-dependent, in addition to the known Z-dependence [29,31,35]. However, such a modification of the model calculation has to take into account that the presently predicted half-life of 33 s for ^{105}Sn decay agrees with experiment ($T_{1/2}$ = 34 (1) s [36]). Clearly, the theoretical calculations have to be extended towards heavier nuclei with special attention paid to the 2 particle-2 hole neutron correlations. So far the core polarization hindrance factors were calculated only for N = 50 isotones and adopted for discussion of GT strength of N > 50 nuclei in the ^{100}Sn region. The discrepancy between predicted and measured half-lives might also be related to the inaccuracies in the

calculated beta transition energies. These deficiencies are presumably bigger for more complex nuclei like ^{102}In and ^{100}Cd than for N=50 or N=51 isotones.

In order to calculate β-delayed proton properties for a comparison with experiment, we used the shell-model GT strength together with a statistical model [37,38]. The justification of the statistical approach can be taken from the fact that the shell model predicts more than 1800 levels in ^{102}Cd with excitation energies between 2 and 8.3 MeV to be populated in the GT β decay of ^{102}In. As can be seen from Table 4, the model calculations underestimate the branching ratios for β-delayed proton emission, if the calculated Q_{EC} and S_p values are used. However, already a small change of these values towards those from experiment or from empirical systematics yields agreement with the measured branching ratios for β-delayed proton emission.

The theoretical proton energy spectra for ^{100}In and ^{102}In decays, generated within a statistical model, are shown in Fig. 4. The spectra correspond to the parameter set presented in Table 4, "Model calculations" part, in the last row of both ^{100}In and ^{102}In sections, respectively. One can see a remarkable agreement between theoretical and detected spectra with respect to the energy ranges of emitted protons as well as to the center of gravity of energy distribution. However, this cannot be considered as a proof of correctness of the input parameters, like β-strength function, since the shape of the proton spectrum is not very sensitive to the used parameters.

5. Conclusions

We have measured β decay properties of the very neutron-deficient isotopes ^{102}In and ^{100}In and have thereby gained information on GT β decay in the region of the doubly magic nucleus ^{100}Sn. The β^+/EC decay of ^{102}In resembles very much that of ^{104}In. In both cases, levels with high excitation energy in the daughter nucleus are directly fed by β^+/EC decay. Subsequent statistical deexcitation of these states, situated in a region of high level density, populates the low-lying levels that have been identified by means of high-resolution discrete γ

spectroscopy. This means that the latter method does not represent a proper tool to investigate the ß strength function of such nuclei which should rather be studied by total absorption gamma spectroscopy (TAGS). There is a clear need to improve the TAGS data for ^{104}In and to measure such data also for lighter odd-A indium isotopes. Results from discrete γ spectroscopy can be used to facilitate the analysis of TAGS data and to get information on the gross structure of the decay.

Even the limited data obtained for the GT decay of ^{102}In and ^{100}In have allowed us to perform a first test of advanced theoretical predictions. These calculations [24] manifest for the first time the experimentally suggested features (see also [2,3]) such as the spreading of the $\pi g_{9/2} \rightarrow \nu g_{7/2}$ GT strength over hundreds of transitions which mainly proceed to high-lying states with excitation energies of 5 to 6 MeV. The total calculated $B_{\Sigma}(GT) = 5$ for the ^{102}In decay is above the experimentally postulated lower limit of 1.0, and the half-life resulting from the model of about 10 s is shorter than the measured value of 22 (1) s. This could be connected to the hindrance factor used in the calculations. This factor originates from a product $h_{cp} \cdot h_{ho}$ of core polarization (calculated for N=50 isotones) and higher order effects hindrance factors, respectively. The calculated hindrance factor is Z- but not N-dependent, which might explain the difference between measured and calculated half-life of ^{102}In and the good agreement between experiment and theory in case of the ^{100}In half-life.

^{102}In is actually the odd-odd nucleus with the largest distance from the doubly-closed-shell core ^{100}Sn where large shell-model calculations of β decay properties do not exceed practical computer limitations. Such calculations without major space truncation are not yet possible, e.g., for ^{104}In whose GT strength distribution has already been studied experimentally by the TAGS method [6].

From the discrete γ spectroscopy an estimate of the energy of the so-called "100 % level" can be given, which amounts to 5.74 MeV for the decay of ^{102}In. Since this level lies above the proton separation energy of ^{102}Cd, ß-delayed proton emission becomes a competing decay mode to ß-delayed γ emission. The experimental data obtained for the ß-delayed proton decay of ^{102}In and ^{100}In have been compared to results from statistical model calculations. This comparison yields further evidence for the resonance-like structure of the GT-strength

function, even though this evidence is not unambiguous in view of the numerous (yet unmeasured) parameters involved in the statisitical-model calculation. One way to improve this situation would be to determine the relevant Q_{EC} and S_p values with higher accuracy, e.g. by measuring positron-proton coincidences as a function of proton energy.

Acknowledgements

The authors B. A. B. and Z. J. would like to acknowledge support from the Alexander von Humboldt Foundation, and (B. A. B.) from NSF grants 90-17077 and 94-03666.

References

1. K. Rykaczewski, Inst. Phys. Conf. Ser. No 132: Section 5, 1993, p.517. Proc. 6th Int. Conf. on Nuclei far from Stability & 9th Int Conf. on At. Masses and Fundamental Constants, Bernkastel-Kues, Germany, 1992
2. J. Vanhorenbeeck, E. Coenen, P. Decrock, P. Dendooven, K. Deneffe, M. Huyse, G. Reusen, P. Van Duppen, J. Wauters and P. del Marmol, Phys. Rev. **C39** (1989) 1528
3. V.R. Bom, R.W. Hollander, E. Coenen, K. Deneffe, P. Van Duppen and M. Huyse, Z. Phys. **A331** (1988) 21
4. J. Blachot, J.P. Husson, J. Oms and G. Berrier, Nucl. Data Sheets, Vol **41** (1984) 53
5. G. Reusen, V.R. Bom, P. Decrock, P. Dendooven, M. Huyse, R.W. Hollander, P. Van Duppen, J. Vanhorenbeeck and J. Wauters, Z. Phys. **A336** (1990) 381
6. L. Batist, V. Wittmann, G. Alkhazov, A. Bykow, H. Keller, R. Kirchner, E. Roeckl, P. Van Duppen, M. Huyse, G. Reusen, A. Płochocki, M. Pfützner, K. Rykaczewski, J. Szerypo, J. Zylicz., GSI Scientific Report 1992, GSI 93-1, p.82, to be submitted to Nucl. Instr. and Meth.
7. R. Kirchner, D. Marx, O. Klepper, V. T. Koslowsky, T. Kühl, P. O. Larsson, E. Roeckl, K. Rykaczewski, D. Schardt, J. Eberz, G. Huber, H. lochmann, R. Menges, G. Ulm, Nucl. Instr. Meth. **A234** (1985) 224
8. J. Tréherne, J. Genevey, A. Gizon, J. Gizon, R. Beraud, A. Charvet, R. Duffait, A. Emsallem and M. Meyer, Z. Phys. **A309** (1982) 135
9. R. Kirchner, Nucl. Instr. Meth. **A292** (1990) 203
10. H. Keller, R. Kirchner, O. Klepper, D. Schardt, R.S. Simon, P. Kleinheinz, C.F. Liang and P. Paris, Nucl. Instr. and Meth. **A300** (1991) 67
11. W.N. Lennard and K.B. Winterbon, Nucl. Instr. Meth. **B24/25** (1987) 1035
12. W.N. Lennard, H. Geissel, K.B. Winterbon, D. Phillips, T.K. Alexander and J.S. Forster, Nucl. Instr. Meth. **A248** (1986) 454

13. E. Browne and R. Firestone, Table of Radioactive Isotopes (1986).

14. H. Keller, R. Barden, R. Kirchner, O. Klepper, E. Roeckl, D. Schardt, I. S. Grant, A. Płochocki, K. Rykaczewski, J. Szerypo and J. Żylicz, Z. Phys. **A339** (1991) 355

15. G. Reusen, PhD thesis, K.U. Leuven (1993)

16. G. Audi and A. H. Wapstra, Nucl. Phys. **A565** (1993) 1

17. J. Blachot, Nucl. Data Sheets **64** (1991) 1

18. W. Kurcewicz, E. F. Zganjar, R. Kirchner, O. Klepper, E. Roeckl, P. Komninos, E. Nolte, D. Schardt, P. Tidemand-Petersson, Z. Phys. **A308** (1982) 21

19. N.B. Gove and M.J. Martin, Nucl. Data Tables **A10** (1971-1972)

20. D. Alber, A. Berger, H.H. Bertschat, H. Grawe, H. Haas, H. Kluge, A. Kuhnert, H.E. Mahnke, K.H. Maier, R. Schubart, B. Spellmeyer, X. Sun and L. Wood, Z. Phys. **A344** (1992) 1

21. D. Alber, H. Grawe, H. Haas, B. Spellmeyer and X. Sun, Z. Phys. **A327** (1987) 127

22. J. Blachot, Nuclear Data Sheets **45** (1985) 701

23. H.-W. Müller and D. Chmielewska, Nuclear Data Sheets **48** (1986) 663

24. B. A. Brown and K. Rykaczewski, "Gamow-Teller strength in the region of ^{100}Sn", to be published

25. M. Huyse, unpublished

26. D. De Frenne, E. Jacobs, M. Verboven and G. De Smet, Nuclear Data Sheets **53**, 73 (1988)

27. J. Blachot, Nuclear Data Sheets **62** (1991) 803

28. H. Keller, PhD thesis, Technische Hochschule Darmstadt (1991)

29. I.S. Towner, Nucl. Phys. **A444** (1985) 402

30. O. Klepper and K. Rykaczewski, preprint GSI-90-63 (1990), published in "Recent Advances in Nuclear Structure", D. Bucurescu, G. Cata-Danil, N. V. Zamfir (Eds.), World Scientific Publ. Comp., Singapore, 1991, p.45

31. I. P. Johnstone, Phys Rev. **C44** (1991) 1476

32. B. A. Brown and B. H. Wildenthal, At. Data and Nucl. Data Tables **33** (1985) 347

33. A. Płochocki et al., Z. Phys. **A342** (1992) 43

34. K. Rykaczewski et al., Z. Phys. **A332** (1989) 176

35. L. D. Skouras and P. Manakos, J. Phys. G.: Nucl. Part. Phys. **19** (1993) 731

36. M. Pfützner, A. Płochocki, K. Rykaczewski, J. Szerypo, J. Żylicz, H. Keller, R. Kirchner, O. Klepper, E. Roeckl, D. Schardt, M. Huyse, G. Reusen, P. Van Duppen and B. A. Brown, GSI Preprint GSI-94-23, April 1994 and Nucl. Phys. (1994), to be published

37. P. Hornshøj, K. Wilsky, P. G. Hansen, B. Jonson and O. B. Nielsen, Nucl. Phys. **A187** (1972) 609

38. B. Jonson, E. Hagberg, P. G. Hansen, P. Hornshøj and P. Tidemand-Petersson, Proc. 3rd Int. Conf. on Nuclei far from Stability, Cargèse, 1976, CERN 76-13, p.277

39. P. De Gelder, E. Jacobs and D. De Frenne, Nuclear Data Sheets **38** (1983) 545

Table Captions

Table 1 : List of ß-delayed γ rays assigned to the decay of ^{102}In. For each γ ray the energy is given in keV and the intensity relative to the 776.5 keV line. All intensities have been derived from singles spectra except for those marked by an asterisk, which have been determined on the basis of coincidence measurements.

Table 2 : List of excitation energies of ^{102}Cd levels together with the "missing intensity" for each level, relative to 776.5 keV line (see text).

Table 3 : Ratios of γ intensities obtained from single and gated spectra for some γ rays from the decay of ^{102}Cd and ^{102}In.

Table 4 : Compilation of β-delayed proton data for the decay of ^{102}In and ^{100}In. Experimental results from this work are confronted to Q_{EC} and S_p values from a recent mass evaluation [16] and to predictions of model calculations (see text). The Q_{EC} values are given for the precursors (^{102}In, ^{100}In), whereas the S_p values are those of the respective daughter nuclei (^{102}Cd, ^{100}Cd). $b_{\beta p}$ indicates the branching ratio for β-delayed proton emission per precursor decay. $b_{\beta p}^{exc}$ represents the branching ratio for proton emission to the first excited state of ^{101}Ag (98 keV) and ^{99}Ag (343 keV), respectively, and is given as a fraction of the corresponding $b_{\beta p}$ value.

Table 1

Energy [keV]	Intensity [%]
157.2 (1)	4.6 (2)
313.7 (2)	7.2 (7)
331.1 (2)	1.7 (4)
397.3 (1)	10.2 (5)
487.8 (1)	3.0 (3)
593.3 (2)	29.5 (4)
749.4 (2)	11.1 (5)
765.6 (2)	3.4 (3)
776.5 (2)	100
794.2 (1)	2.0 (2)
822.4 (2)	4.7 (4)*
861.5 (4)	92 (5)*
923.2 (2)	19.2 (8)
1236.4 (1)	3.8 (4)*
1258.8 (4)	2.8 (2)*

Table 2

Energy [keV]	Missing Intensity [%]
776.5	5 (5)
1628.0	15 (5)
2035.3	11.0 (6)
2231.3	20.1 (8)
2387.4	11.1 (5)
2403.6	3.4 (3)
2561.8	9.1 (12)
2719.1	7.6 (4)
2829.5	2.0 (2)
2874.9	11.0 (8)
3053.7	4.7 (4)

Table 3

^{102}Cd		^{102}In	
Energy [keV]	$\frac{\text{singles}}{\text{coinc.}}$	Energy [keV]	$\frac{\text{singles}}{\text{coinc.}}$
97.4	150 (7)	397.3	13.6 (5)
116.0	101 (2)	593.3	14.3 (3)
213.3	92 (3)	749.4	14.7 (6)
360.6	81 (4)	776.5	15.3 (2)
414.8	72 (2)	822.4	23 (3)
481.0	220 (2)	923.2	15.3 (5)
675.7	117 (7)		

Table 4

	Experiment (this work)						Model calculations (this work)			
Precursor	$T_{1/2}$ [s]	Number of observed p-X and p-γ coincidence events	$b_{\beta p}$	$b^{exc}_{\beta p}$ [%]	$\left(\frac{\beta^+}{\beta^+ + EC}\right)_{\beta p}$	Q_{EC} range [MeV]	Q_{EC} [MeV]	S_p [MeV]	$b_{\beta p}$	$b^{exc}_{\beta p}$ [%]
^{102}In	22 (1)	Cd K X rays (38), 98.1 keV (6), 511 keV (1)	9.3 (13) $\cdot 10^{-5}$	19 (9)	0.07 (7)	8.6-9.9	8.73[c]	5.59[c]	$8.4 \cdot 10^{-6}$	~ 10
							8.73[c]	5.48 (12)[a]	$(1.6^{+2.1}_{-0.8}) \cdot 10^{-5}$	~ 10
							8.90 (33)[a]	5.48 (12)[a]	$(3.5^{+5.5}_{-1.2}) \cdot 10^{-5}$	~ 10
^{100}In	6.1 (9)	Cd K X rays (2), 511keV (2)	$> 3.9 \cdot 10^{-2}$	-	$0.80^{+0.14}_{-0.11}$	9.3-12.5	10.05[c]	5.0[c]	$7 \cdot 10^{-3}$	~ 4
							10.5 (4)[b]	4.83 (19)[a]	$(6^{+4}_{-3}) \cdot 10^{-2}$	~ 4

a) experimental values [16], b) values obtained by extrapolation of empirical systematics [16], c) value calculated within shell-model [24].

Figure Captions

Fig. 1 γ ray spectra measured at mass 102 by using (a) the FEBIAD ion source with an implantation-decay cycle of 48 s, and (b) the thermal ion source. When measuring spectrum (b), the mass-102 beam was continuously implanted in front of the detector. Therefore, ^{102}Cd and ^{102}Ag lines appear in the spectrum as daughter and granddaughter activity of ^{102}In decay, whereas in the spectrum (a), measured at moving-tape collectors, these grow-in effects are negligible. The most prominent γ lines from the decay of ^{102}In, ^{102}Cd and ^{102}Ag are marked by "In", "Cd" and "Ag", respectively. The lines indicated by a cross belong to the room background.

Fig. 2 Level scheme of ^{102}Cd (a) from this work and (b) from an in-beam study [8]. The energy unit is keV.

Fig. 3 The ß spectrum of ^{102}In recorded with the summation-free $ß^+$-endpoint spectrometer.

Fig. 4 Energy spectra of β-delayed protons from the decay of ^{102}In (a) and ^{100}In (b). The spectra were obtained by coincident summing of pulses from the ΔE and E detectors. A low-energy threshold is imposed on these spectra due to the fact that, depending on the angle of incidence, protons with energies up to 1 MeV and 2 MeV, respectively, are stopped in the ΔE detector. The theoretical proton spectra are represented by a dashed histogram.

Fig. 5 Low-energy γ ray spectrum recorded in coincidence with β-delayed protons from ^{102}In.

Fig. 6 Systematics of the low-energy part of the level schemes of even-even cadmium isotopes with masses ranging from 100 to 110. The data have been taken from refs. [22,23] (^{100}Cd), this work (^{102}Cd), refs. [2] (^{104}Cd), [26] (^{106}Cd), [27] (^{108}Cd) and [39]

(^{110}Cd).

Fig. 7 The ß strength function in bins of 500 keV excitation energy for the decay of ^{100}In - ^{108}In. The height of each bar is equal to the sum of B(GT) within the 500 keV interval. The experimental strength functions (solid histogram) have been determined from the γ intensity balance except for ^{104}In where the result from the deconvolution of the TAGS spectrum is given (shaded area represents an error range for each bin). The excitation energy of the "100 % level" is indicated by a solid bar, its height gives the corresponding B(GT). Both the $\log(ft)_{\Sigma}$ and the $\log(ft)_{100}$ are given. For ^{100}In and ^{102}In the theoretical B(GT) predictions [24] (dashed histogram) are shown. The Q_{EC} values are taken from the mass evaluation [16] (^{102}In, ^{104}In, ^{106}In, ^{108}In) or from this work (^{100}In).

Fig. 8 The summed GT-strength, $B_{\Sigma}(GT)$, for the decay of nuclei in the neighborhood of ^{100}Sn (for ^{102}In only the lower limit, derived from the "100% level" value of $1.4^{+0.5}_{-0.4}$, is given). The decay data are taken from refs: [1,6] (^{104}In), [26] (^{106}In), [27] (^{108}In) and [30] (even-even nuclei).

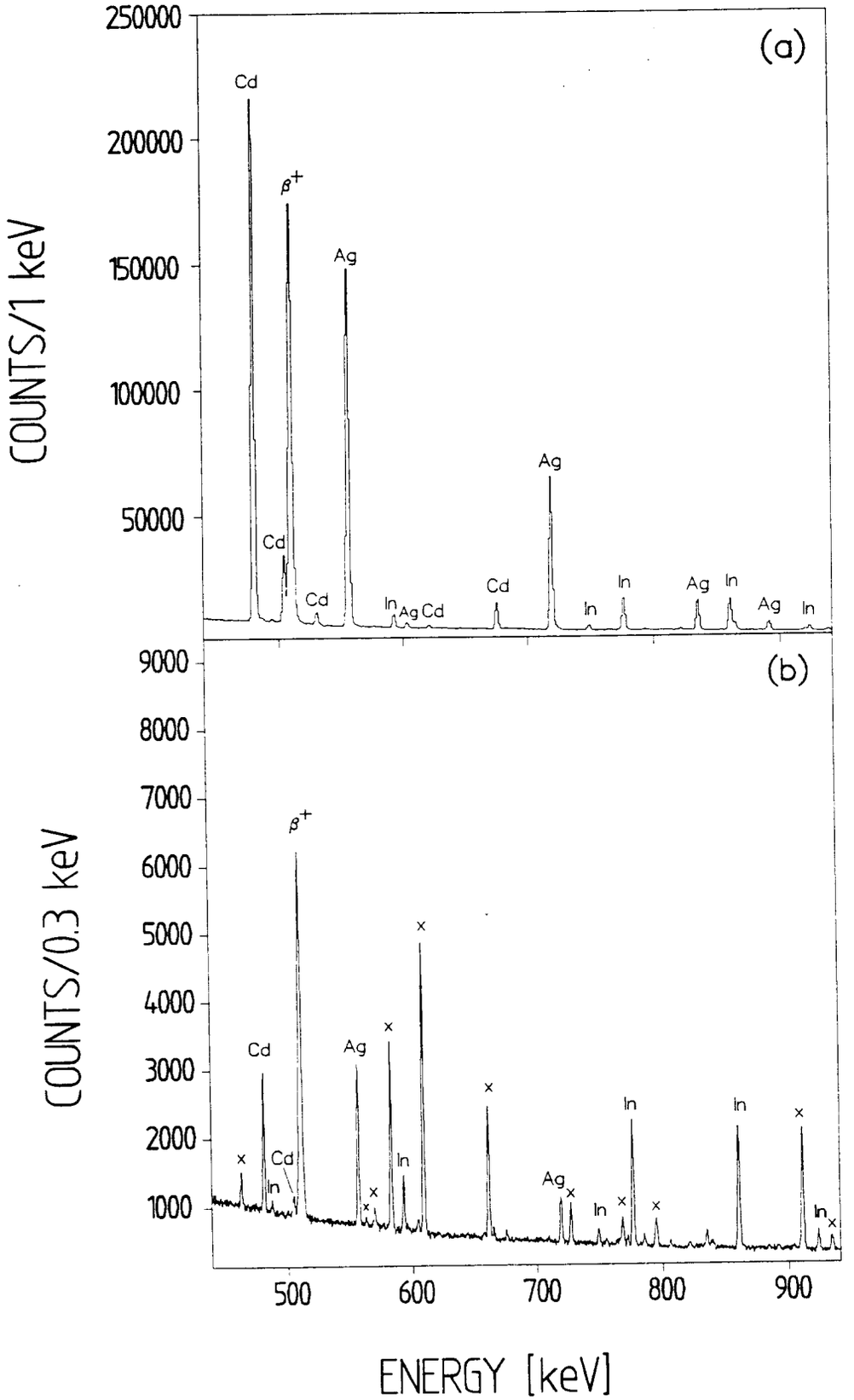
(a)
(b)
COUNTS/1 keV
COUNTS/0.3 keV
ENERGY [keV]
250000
200000
150000
100000
50000
9000
8000
7000
6000
5000
4000
3000
2000
1000
500
600
700
800
900
Cd
Ag
In
β+
×

Fig. 2

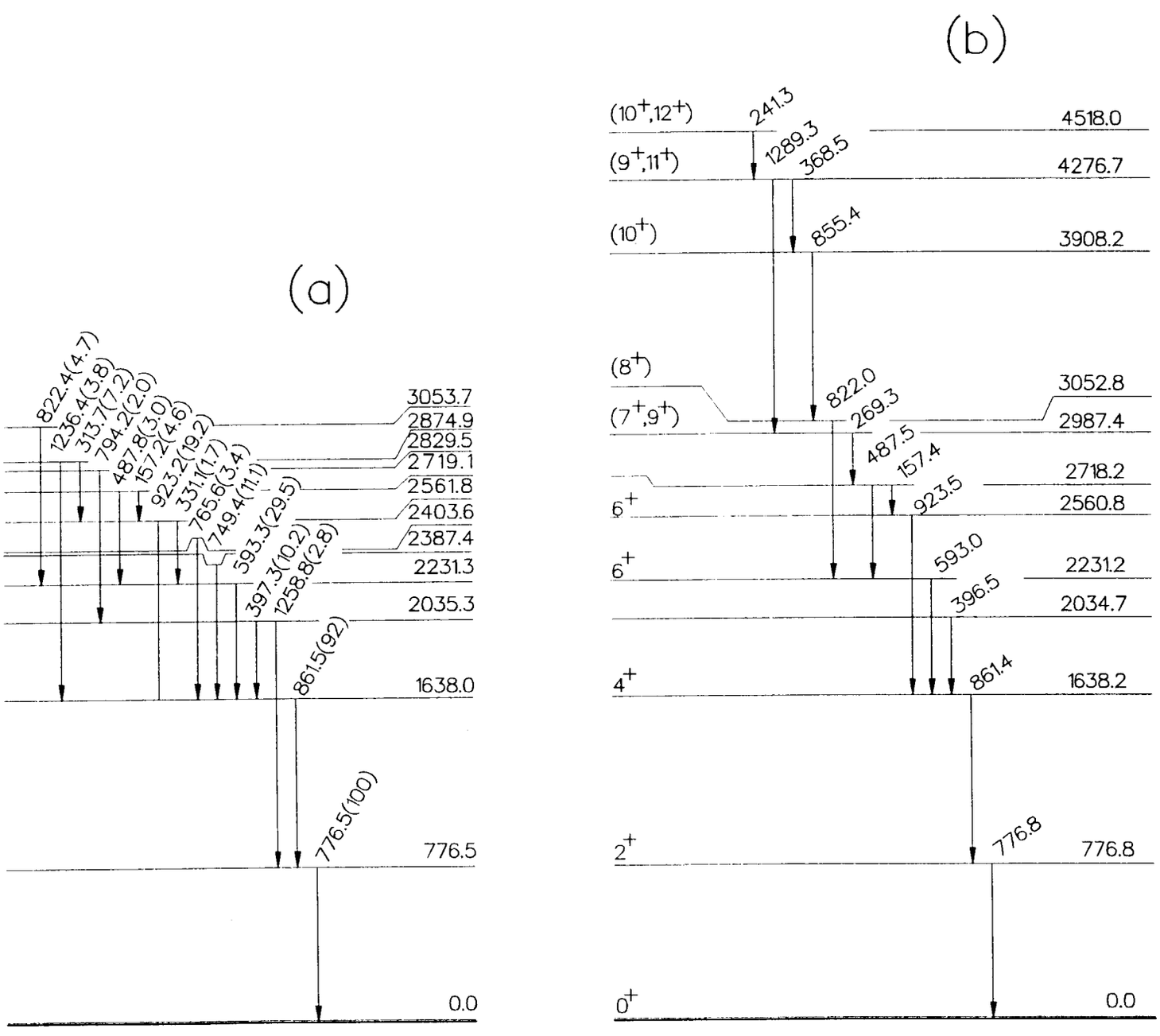
(a)
822.4(4.7)
1236.4(3.8)
313.7(7.2)
794.2(2.0)
487.8(3.0)
157.2(4.6)
923.2(19.2)
331.1(1.7)
765.6(3.4)
749.4(11.1)
593.3(29.5)
397.3(10.2)
1258.8(2.8)
861.5(92)
776.5(100)
3053.7
2874.9
2829.5
2719.1
2561.8
2403.6
2387.4
2231.3
2035.3
1638.0
776.5
0.0
(b)
(10+,12+)
(9+,11+)
(10+)
(8+)
(7+,9+)
6+
6+
4+
2+
0+
241.3
1289.3
368.5
855.4
822.0
269.3
487.5
157.4
923.5
593.0
396.5
861.4
776.8
4518.0
4276.7
3908.2
3052.8
2987.4
2718.2
2560.8
2231.2
2034.7
1638.2
776.8
0.0

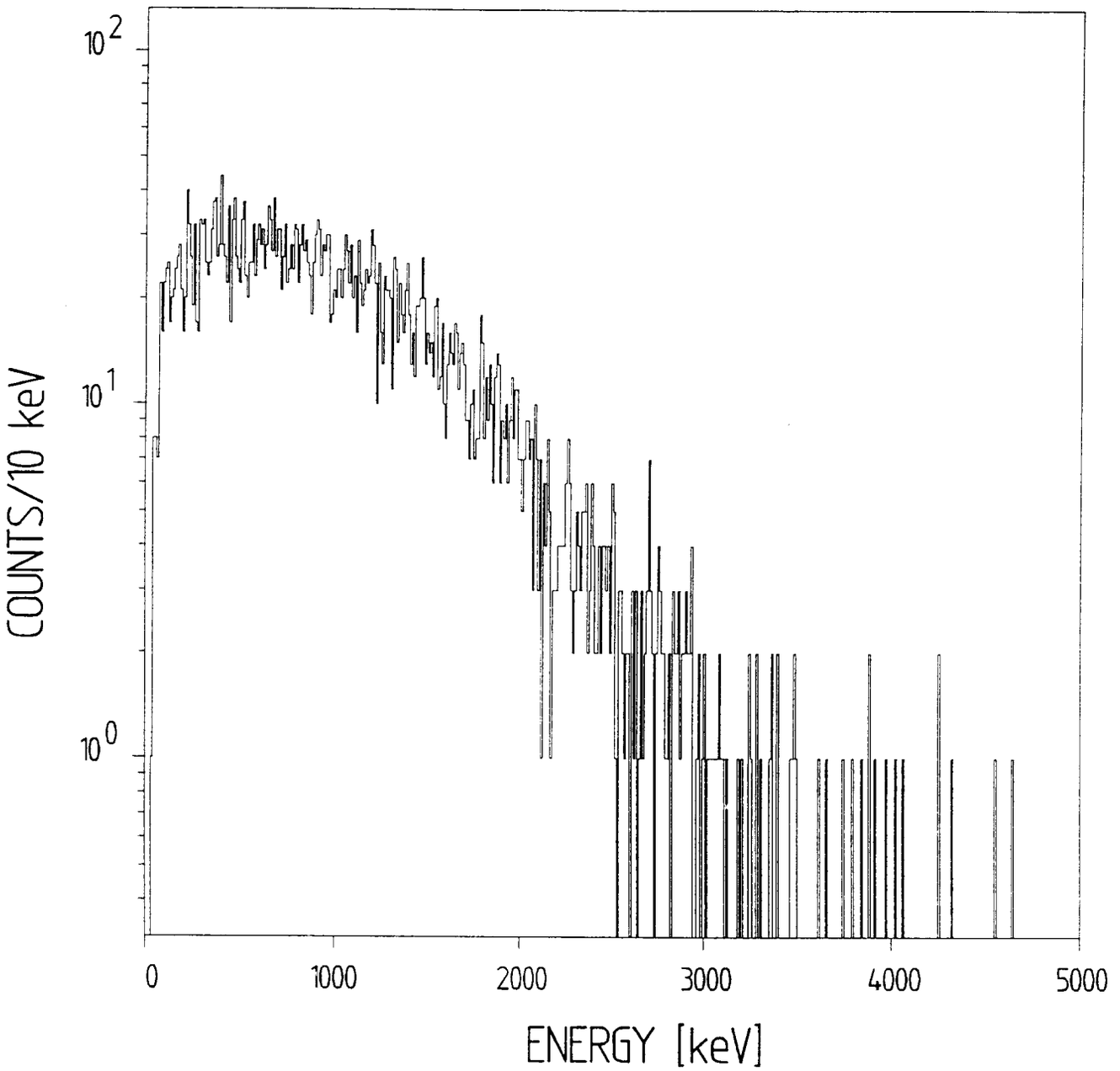
10^2
10^1
10^0
COUNTS/10 keV
0
1000
2000
3000
4000
5000
ENERGY [keV]

Fig. 3

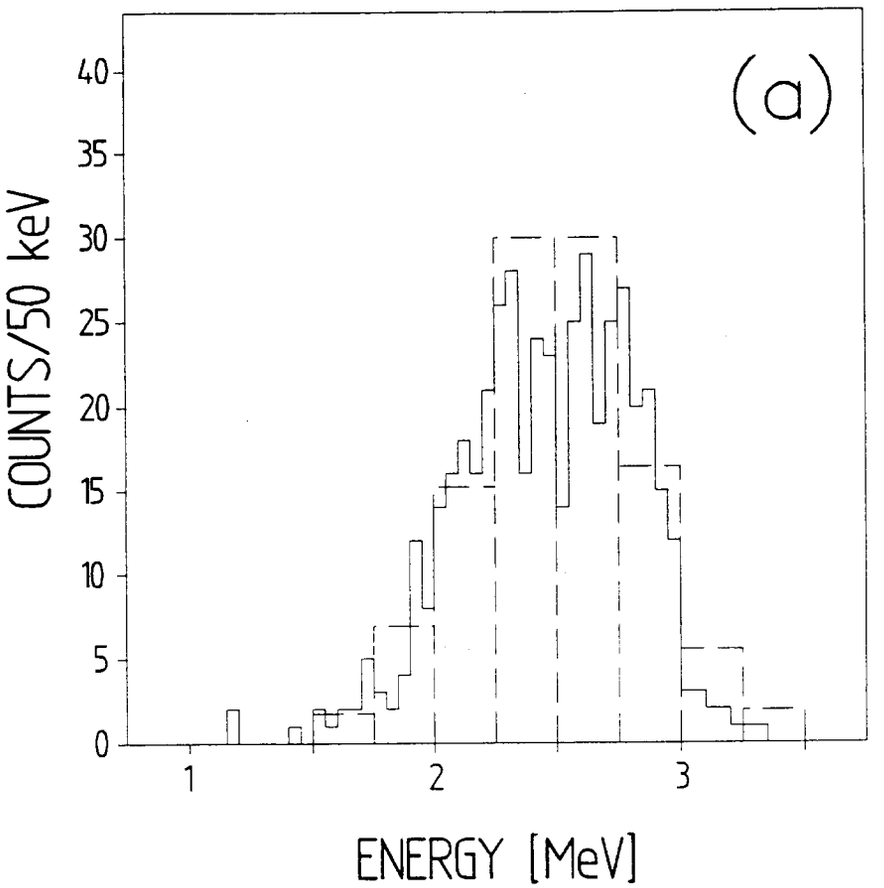
(a)
COUNTS/50 keV
0
5
10
15
20
25
30
35
40
1
2
3
ENERGY [MeV]

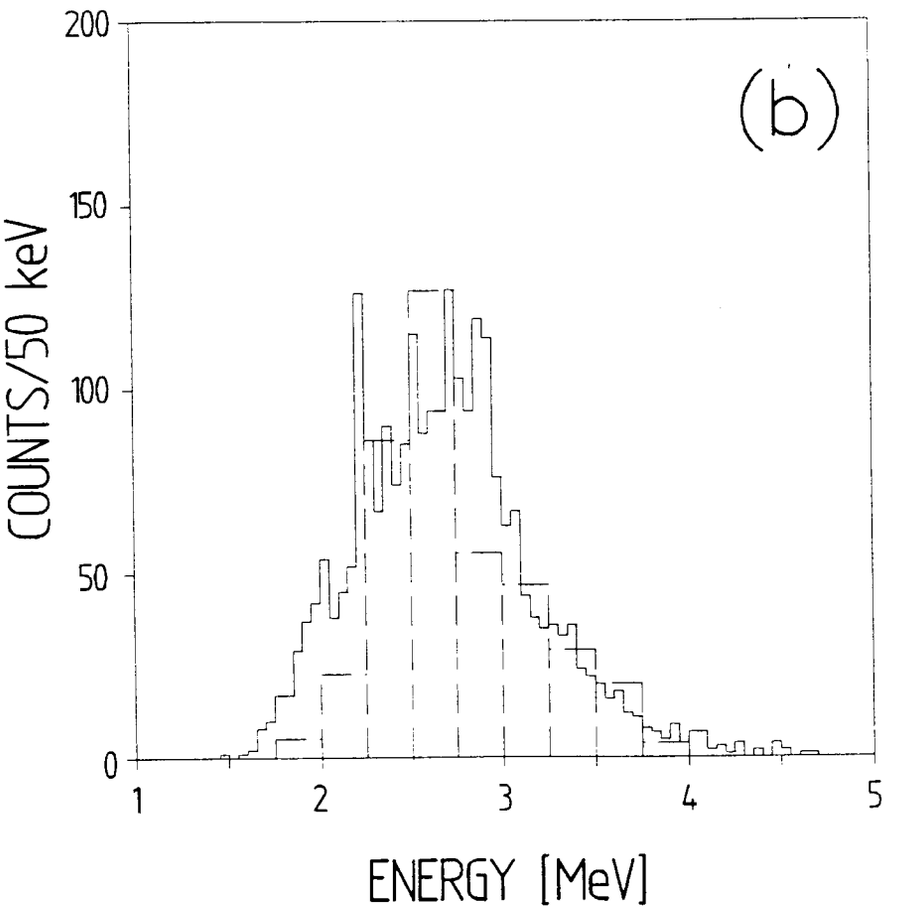
(b)
COUNTS/50 keV
0
50
100
150
200
1
2
3
4
5
ENERGY [MeV]

Fig. 4

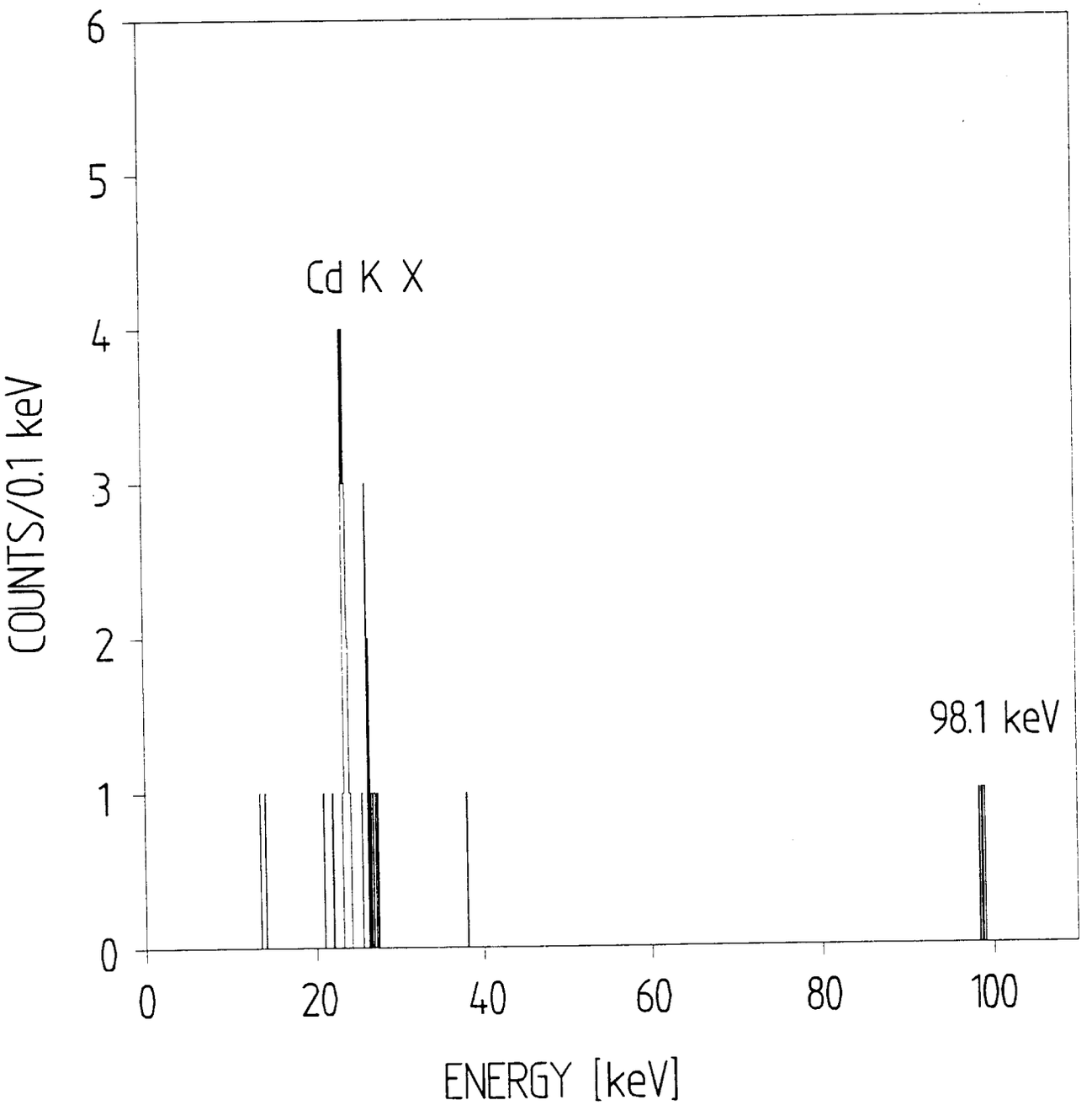

Fig. 5

Fig. 9

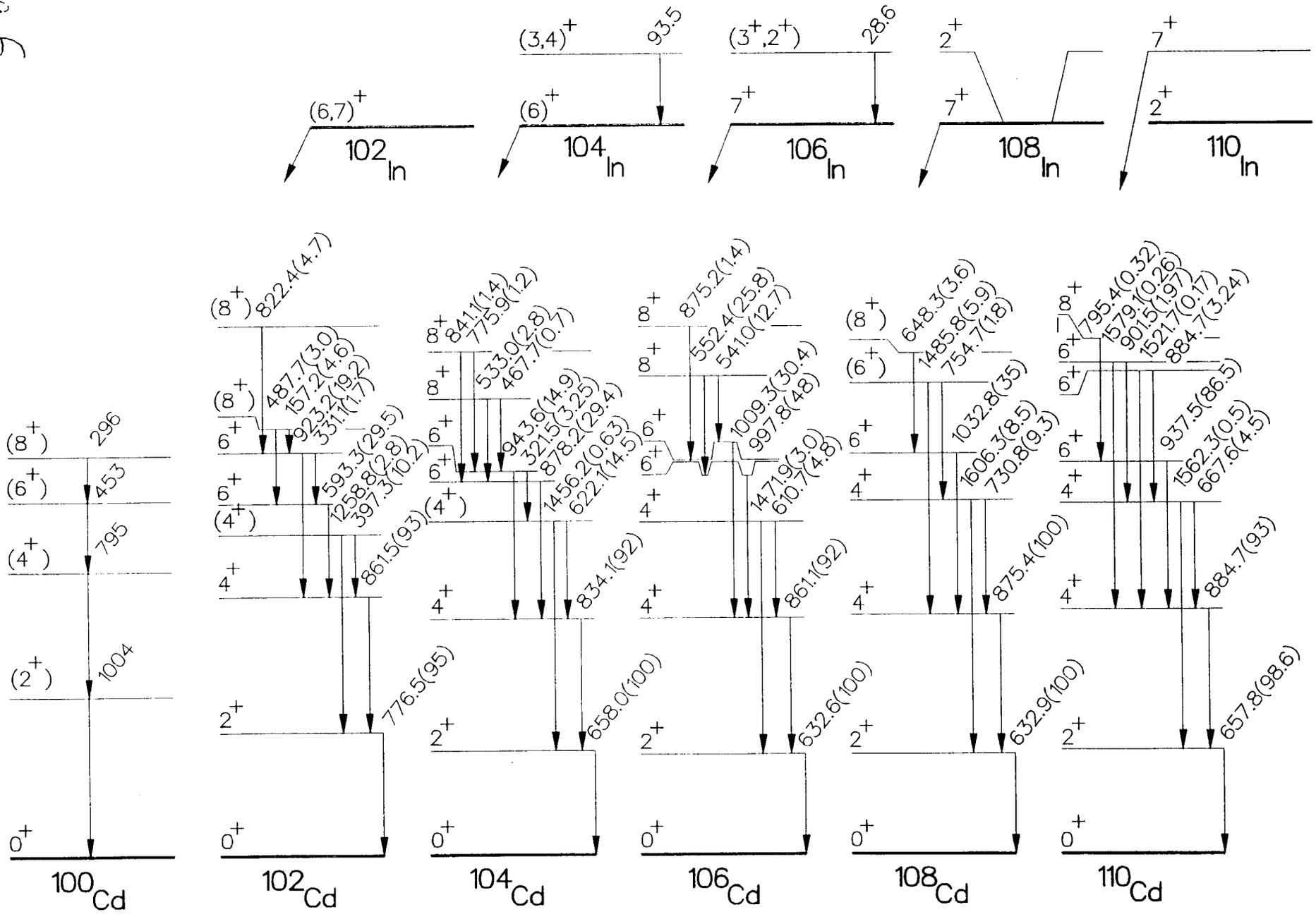
(6,7)+
102In
(3,4)+
93.5
(6)+
104In
(3+,2+)
28.6
7+
106In
2+
7+
108In
7+
2+
110In
(8+)
296
(6+)
453
(4+)
795
(2+)
1004
0+
100Cd
(8+)
822.4(4.7)
(8+)
487.7(3.0)
157.2(4.6)
923.2(19.2)
331.1(1.7)
6+
6+
593.3(29.5)
1258.8(2.8)
397.3(10.2)
(4+)
861.5(93)
4+
776.5(95)
2+
0+
102Cd
8+
841.1(1.4)
775.9(1.2)
8+
533.0(2.8)
467.7(0.7)
6+
943.6(14.9)
321.5(3.25)
878.2(29.4)
6+
1456.2(0.63)
622.1(14.5)
(4+)
4+
834.1(92)
2+
658.0(100)
0+
104Cd
8+
875.2(1.4)
8+
552.4(25.8)
541.0(12.7)
6+
1009.3(30.4)
997.8(48)
6+
1471.9(3.0)
610.7(4.8)
4+
861.1(92)
2+
632.6(100)
0+
106Cd
(8+)
648.3(3.6)
1485.8(5.9)
754.7(1.8)
(6+)
6+
1032.8(35)
1606.3(8.5)
730.8(9.3)
4+
875.4(100)
2+
632.9(100)
0+
108Cd
8+
795.4(0.32)
1579.1(0.26)
901.5(1.97)
1521.7(0.17)
884.7(3.24)
6+
6+
937.5(86.5)
6+
1562.3(0.5)
667.6(4.5)
4+
884.7(93)
2+
657.8(98.6)
0+
110Cd

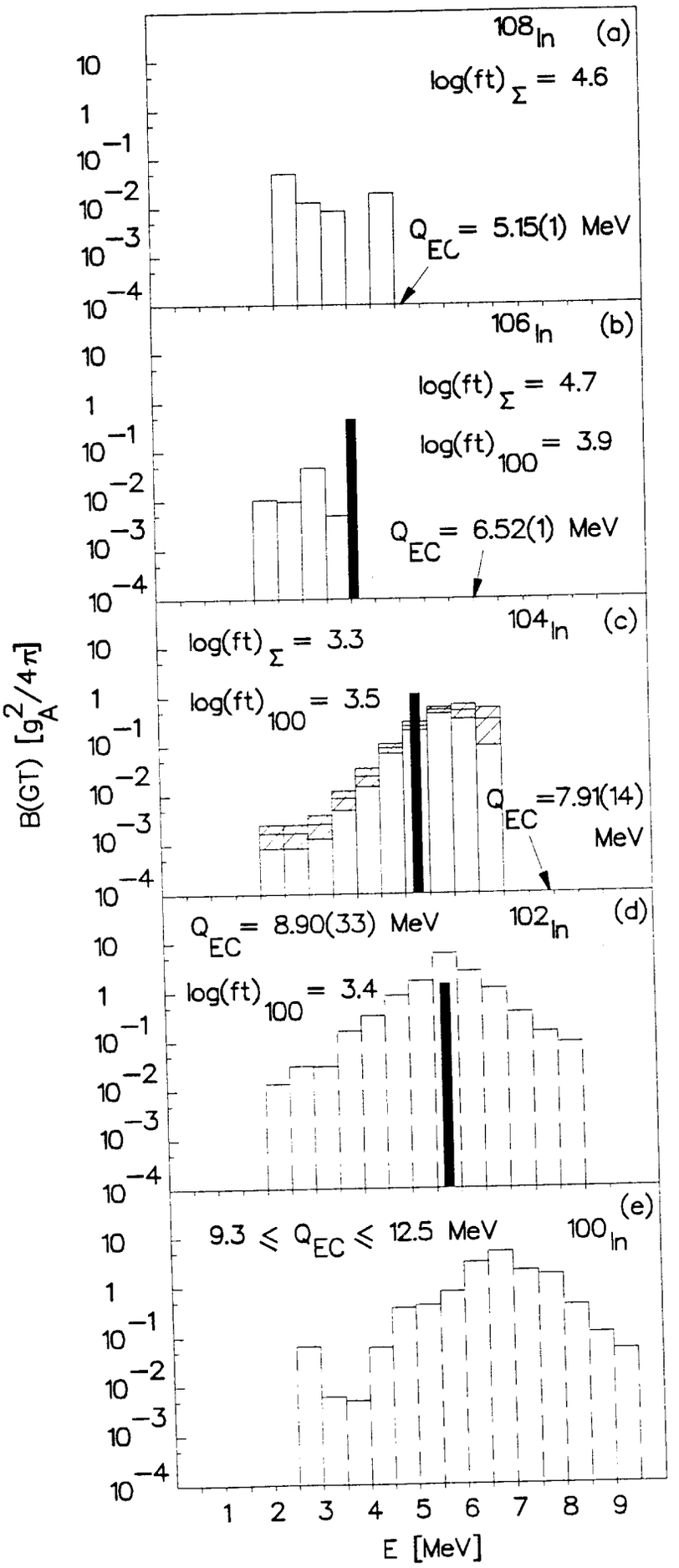
^{108}In (a)
log(ft)$_\Sigma$ = 4.6
Q_{EC} = 5.15(1) MeV
^{106}In (b)
log(ft)$_\Sigma$ = 4.7
log(ft)$_{100}$ = 3.9
Q_{EC} = 6.52(1) MeV
^{104}In (c)
log(ft)$_\Sigma$ = 3.3
log(ft)$_{100}$ = 3.5
Q_{EC} =7.91(14) MeV
^{102}In (d)
Q_{EC} = 8.90(33) MeV
log(ft)$_{100}$ = 3.4
^{100}In (e)
9.3 ≤ Q_{EC} ≤ 12.5 MeV
B(GT) [$g_A^2/4\pi$]
E [MeV]

Fig. 7

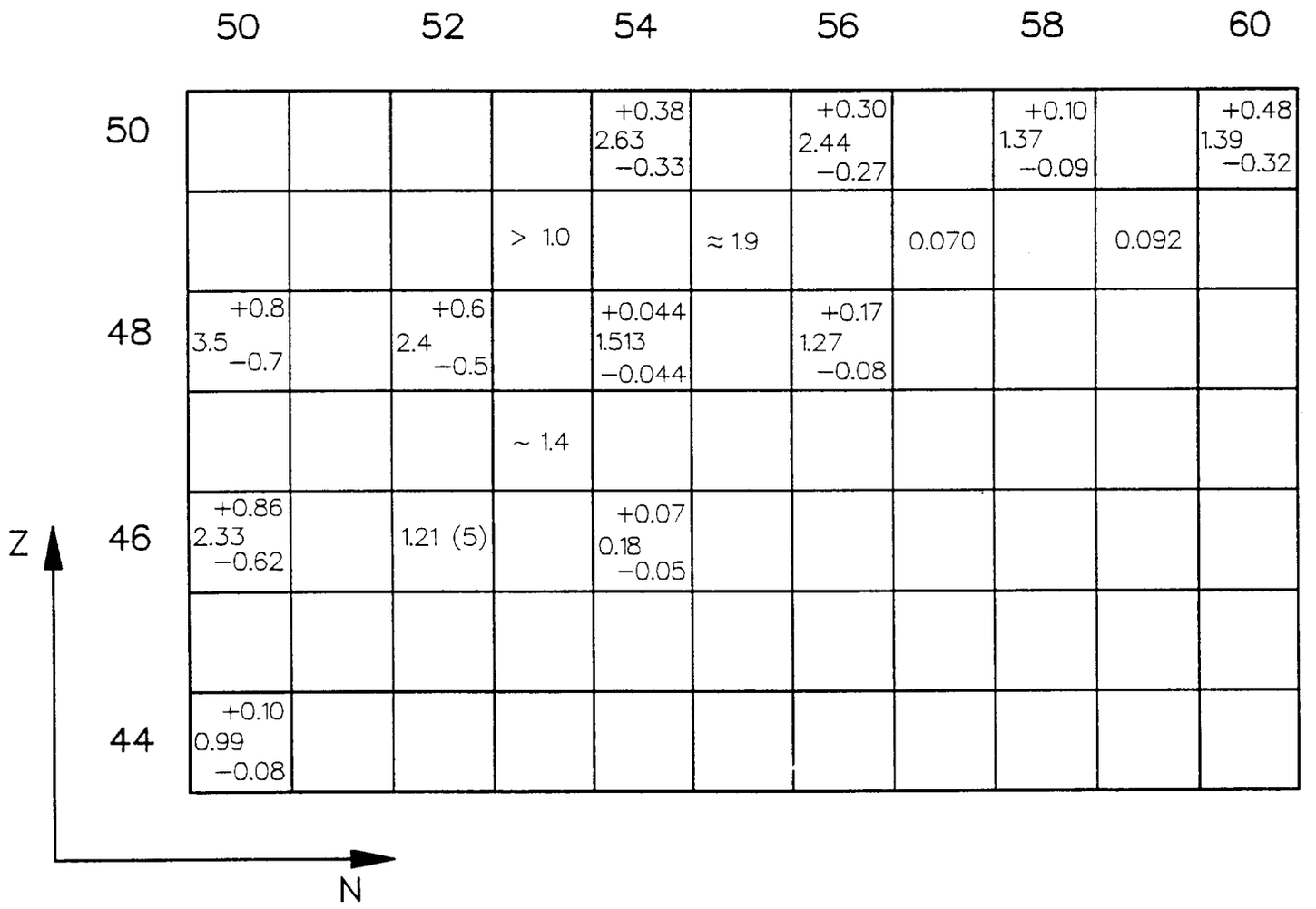
50
52
54
56
58
60
50
48
46
44
+0.38
2.63
−0.33
+0.30
2.44
−0.27
+0.10
1.37
−0.09
+0.48
1.39
−0.32
> 1.0
≈ 1.9
0.070
0.092
+0.8
3.5
−0.7
+0.6
2.4
−0.5
+0.044
1.513
−0.044
+0.17
1.27
−0.08
~ 1.4
+0.86
2.33
−0.62
1.21 (5)
+0.07
0.18
−0.05
+0.10
0.99
−0.08
Z
N

Fig. 8